Off-Critical Phase Separation and Gelation in Solutions of Gelatin and Dextran

R. H. Tromp* and R. A. L. Jones

Polymer and Colloids Group, Cavendish Laboratory, University of Cambridge, Madingley Road, Cambridge CB3 0HE, United Kingdom

Received May 3, 1996; Revised Manuscript Received September 9, 1996[⊗]

ABSTRACT: The phase separation kinetics have been studied with Small angle light scattering (SALS) in strongly asymmetric aqueous mixtures of gelatin and dextran, above and below the gelation temperture of gelatin. The focus is on solutions with gelatin as the majority component. The phase separation gives rise to a distribution of dextran-rich spheres in a gelatin-rich matrix. The SALS pattern shows a maximum, which was interpreted as being due to the interplay between the scattering from dextran-rich nuclei and a surrounding layer depleted in dextran (depletion layer). The size and concentration of the spherical nuclei and their depletion layers were followed in time at temperatures above and below the gelation temperature of the matrix. The results show a strong and complex dependence on temperature and total polymer concentration of the separation kinetics.

Introduction

A detailed knowledge of the phase separation process in aqueous biopolymer systems is important for optimizing the applicability of biological materials in an increasing number of areas. Examples are the morphology of starch based products,[1] synthetic biomembranes,[2] and the texture of processed food.[3] One of the questions that can be raised in this context is to what extent biopolymer mixtures behave like better defined and more controllable mixtures of synthetic polymers. In particular, the tendency of many biopolymers to gel at a certain temperature and at sufficient concentration was shown to strongly influence the kinetics of phase separation in a gelatin/dextran/0.5 M NaCl system and to challenge existing theoretical approaches.[4] Gelation rules out hydrodynamics as a factor determining phase separation kinetics, introducing a time regime, prior to complete freezing, where molecular diffusion is dominating the coarsening of the texture. In this stage the gelation can be regarded as introducing quenched disorder. Recently published numerical results[5] describing spinodal decomposition combined with quenched disorder show morphologies and scattering patterns that are similar to experimental findings in near-critical gelling dextran/gelatin systems. On the other hand, as long as no gelation takes place, phase separation proceeds largely as observed in mixtures of synthetic polymers. The main deviation that was found from the usual behavior, i.e. poor dynamic scaling after long times, can probably be ascribed to polydispersity, which is another common feature of biopolymers.

When gelation takes place simultaneously with phase separation, the immobility of the gelling component will inhibit the separation process and eventually halt it completely. The morphology that has been reached by that time is a function of the gelation rate relative to the separation rate. In gelatin/dextran/water systems, these two rates are comparable, and a change in temperature as small as 1 °C can result in significantly different final morphologies of the mixed gel. Gelation inhibits coarsening, but not to the same extent on all distance scales. It might even stimulate phase separation on small length scales, due to the effectively increasing molecular weight during gelation, which enhances the driving force for phase separation. For example, in near critical mixtures of dextran and gelatin it was found that the lower the temperature (i.e. the faster the gelation), the more intense the higher angle ($q > 2\ \mu m^{-1}$) light scattering. This implies the presence of more inhomogeneities in the concentration on small length scales. Eventually, the kinetics of all phase separation is arrested by the gelation, which stabilizes the mixture by adding an elastic term to the free energy (see ref 6).

In contrast with those in the previous work, the results presented here were obtained from solutions with compositions that are well off-critical and containing much more gelatin that dextran: 0.5% dextran/9.2% gelatin (w/w) and 0.9% dextran/7.2% gelatin (w/w). *Gelatin*-rich off-critical dextran/gelatin systems, on which the present work focuses, are, after phase separation, a spatial distribution of dextran-rich spherical or nearly spherical regions in a gelled gelatin-rich matrix. The spherical regions are all of comparable size. However, *dextran*-rich off-critical systems, which will not be considered any further in this report, form suspensions of gelled gelatin-rich spheres in a fluid dextran-rich solution, where after longer times the gelatin spheres form open clusters. An understanding of the kinetics of growth of the spheres and their clustering might be relevant from a technological point of view because a simple, cheap, and quick way is provided of making an aqueous suspension of relatively monodisperse spherical particles. As will be shown, the off-critical dextran/gelatin systems offer a good opportunity to study quantitatively several aspects of the development of minority phase nuclei during the phase separation. An important reason for their suitability is the small difference in refractive index (Δn) between gelatin and dextran solutions below concentrations of 10%. A small value of Δn renders multiple scattering corrections unimportant and, in the case of the particle size found in the present systems, Rayleigh−Gans scattering theory applicable.

The interpretation of the scattering data from the off-critical dextran/gelatin aqueous systems uses the basic

* Present address of corresponding author: Institute of Food Research, Norwich Research Park, Colney Lane, Norwich NR4 7UA, United Kingdom.

[⊗] Abstract published in *Advance ACS Abstracts,* October 15, 1996.

S0024-9297(96)00656-0 CCC: $12.00

ideas brought forward in previous work on the salt-induced clustering of small (nanometer sized) polystyrene spheres[7] and the crystallization of the minority phase in doped semiconductor glasses.[8] As in the present dextran/gelatin mixture, in these systems isolated nuclei of minority phase are formed, which in many cases are accompanied by a ring in the 2-D scattering pattern. Usually, such a ring is associated with "spinodal decomposition"; i.e. the formation of two interpenetrating phase volumes, the morphology of which is characterized by a certain length, roughly inversely proportional to the position of the ring in reciprocal space. However, as is pointed out in ref 7, the situation of a growing minority phase nucleus, which is surrounded by a layer depleted in minority compound (diffusion limited growth), will also give rise to a ring in the 2-D scattering pattern. The vanishing scattering intensity at an angle with the incident beam that approaches zero, which is not observed in a dilute suspension of spheres in a homogeneous medium, is in that case due to the cancellation of the scattering by the dense nucleus and the dilute depletion layer. Compared with the near-critical "spinodal decomposition", in the off-critical situation with isolated phase regions, it appears to be easier to model the morphology of the phase-separating system in terms of sizes and densities of the nuclei and the depletion layers.

Theory

General. The theory of off-critical and critical phase separation is treated comprehensively in several reviews.[9] Therefore, only a short account will be given here. The onset of phase separation in strongly asymmetrical mixtures is best pictured as being due to the existence of fluctuations in the concentration of a minority compound. When a fluctuation is large enough, the volume/area ratio is sufficient to make growth energetically favorable. In the separation of liquids or solutions, this growth will be diffusion-rate limited in all except the very early stages after the formation of growing fluctuations (nucleation). A concentration gradient will develop around the growing nucleus. Because this layer is depleted in the minority compound, this layer is called the depletion layer. During this diffusion-limited growth of isolated phase particles, the average size R of the particles is usually expected to follow a power-law with a power of $^1/_2$:

$$R = \lambda t^{1/2} \tag{1}$$

After longer times, the depletion layers extend so far that they start to touch those of neighboring particles, and the growth slows down, entering a transition regime where power-law exponents are predicted between $^1/_6$ and $^1/_3$. By the end of the transition regime, the morphology starts to coarsen, i.e. the supersaturation virtually disappears and small nuclei, with relatively highly curved surfaces, start to evaporate to the benefit of larger regions that have less strongly curved surfaces. Several theories to describe this complicated situation have been developed and computer simulations carried out, the predictions of which mainly differ on the point of the growth rate and the size distribution. However, they generally agree that R should follow a power-law with a power of $^1/_3$:

$$R = \alpha t^{1/3} \tag{2}$$

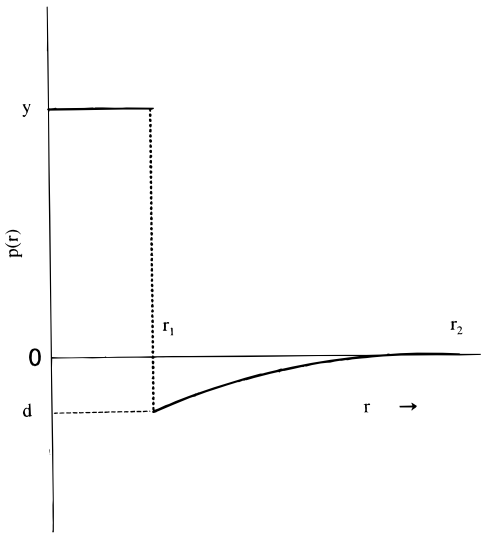

Figure 1. Example of the model profile. The depth d of the depletion layer is strongly exaggerated. The radially weighted integral is forced to zero during the fit.

α and λ (in eq 1) depend on supersaturation, diffusion constant, and the surface tension between the two phases.

Knowledge of shape of the distribution of the particle sizes is important for a quantitative interpretation of the light-scattering pattern of the phase-separating system. Theories trying to describe the evolution of the distribution need the initial distribution, immediately after nucleation. This initial distribution is in general unknown, and the interpretation of scattering patterns in early stages is therefore difficult without extra assumptions. In late stages, dynamic scaling is predicted, i.e, although the individual particle are growing or shrinking, the shape of the distribution becomes independent of time:

$$I(q;t) \sim R_{sc}(t)^3 F[qR_{sc}(t)] \tag{3}$$

$I(q;t)$ is the scattering intensity, q is the absolute value of the scattering vector, $R_{sc}(t)$ is a time dependent characteristic length scale, and $F(x)$ is an universal function, the shape of which depends on the volume fraction of the minority phase, but not on time. The characteristic length $R_{sc}(t)$ grows with time and its reciprocal value corresponds to the position of a peak in the scattering pattern. Dynamic scaling was observed many times in near-critical systems, but less commonly in off-critical systems. In the present off-critical dextran/gelatin system, it was not observed either, possibly because of extreme slowing down of the separation process ("pinning down" effect[10]), even above the gelation temperature. Therefore, the evolution of the scattering pattern was interpreted using more basic considerations.

The Model. The model (Figure 1) used to analyze the scattering pattern was based on two assumptions: (i) the dextran-rich regions that form during the phase separation have a spherical shape and (ii) the enrichment in dextran in the dextran-rich spheres is balanced by an equal depletion of dextran in a shell (depletion layer) concentric with the sphere. The assumption of a spherical shape is the most obvious one for the domain shape in off-critical liquid−liquid phase separation and is supported by microscope photographs (Figure 2), in which the resolution is just sufficient to distinguish

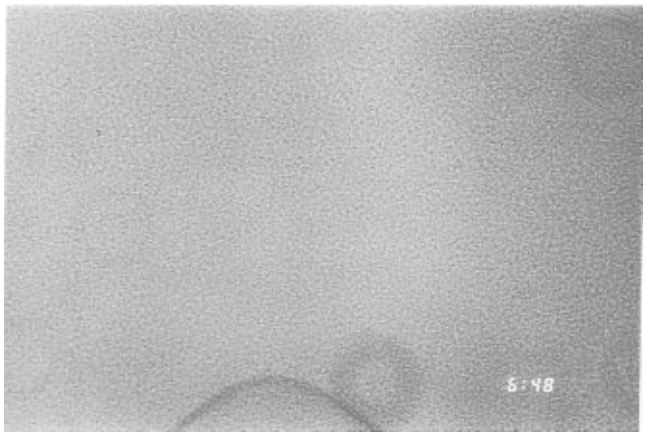

Figure 2. Phase contrast photograph of a 1% dextran/9% gelatin mixture about 10 min after the onset of phase separation. The area of the image is 640 × 480 μm. The number in the corner should be ignored.

spherical phase domains. The second assumption is a formulation of the law of conservation of mass. Three-parameter fits to the data were carried out of the Fourier transform of the concentration profile shown in Figure 1. This profile was used because it meets the condition of mass conservation without invoking any structural detail for which a more complete knowledge is necessary of the nucleation and diffusion processes. The profile $p(r)$ consists of a block-shaped concentration profile of the dextran-rich sphere, of density y, which is proportional to the absolute value of the difference in refractive index of the gelatin and dextran phases, and radius r_1 surrounded by a depletion layer with depth d. In theory, the depth of the depletion layer asymptotically approaches zero at large distances from the center of the sphere. It is expected that a hyperbolic function mimics such a dependence. Indeed, such a shape gave slightly better fits than a straight line. Because implementation of the model needs a finite thickness of the depletion layer, a parameter r_2 was introduced, which is the distance where the hyperbole, after taking the value d (which is negative) at r_1, passes through zero. Consequently, the model profile applied was

$$\begin{aligned} p(r) &= y && \text{for } 0 \le r \le r_1 \\ p(r) &= \frac{r_1 r_2 d}{(r_2 - r_1)r} - \frac{r_1 d}{r_2 - r_1} && \text{for } r_1 < r \le r_2 \\ p(r) &= 0 && \text{for } r > r_2 \end{aligned} \tag{4}$$

where the value of d is imposed by the conservation of mass and therefore a function of y, r_1, and r_2:

$$d = \frac{2y{r_1}^2(r_2 - r_1)}{3r_2({r_2}^2 - {r_1}^2) - 2({r_2}^3 - {r_1}^3)} \tag{5}$$

This expression is derived by setting the radially weighted integral of eq 4 equal to 0. Due to the sharp boundary of the nuclei, the model profile predicts a q^{-4} tail at high values of q. Experimentally, only the first-order maximum can be observed and therefore not the asymptotic q^{-4} behavior of the series of higher order maxima. To include the effect of interference with neighboring particles it was assumed, considering that the volume fraction of dextran spheres is smaller than 0.15, that the pair correlation function $g(r)$ of a dilute hard sphere gas could be used, i.e. $g(r) = 1$ for $r > r_c$ and $g(r) = 0$ for $r < r_c$, where r_c is the distance of closest approach, which was assumed to be equal to r_1. The scattering intensity can then be expressed as follows:

$$I(q) \sim P(q)\, S(q) \tag{6}$$

where the form factor

$$P(q) = \left[\frac{4\pi}{q}\int_0^{r_2} p(r) r \sin(rq)\, \mathrm{d}r\right]^2 \tag{7}$$

and the structure factor $S(q)$ is expressed by

$$S(q) = 1 + \frac{4\pi N}{q}\int_0^{\infty} [g(r) - 1] r \sin(qr)\, \mathrm{d}r \tag{8}$$

where N is the number of particles per unit volume. N was held constant during the fit and estimated from the ratio of the weight fractions of dextran and gelatin:

$$N \approx \frac{3\varphi}{4\pi {r_1}^3} \tag{9}$$

in which φ is the dextran fraction of the total weight of dissolved dextran and gelatin.

Polydispersity of the spheres was ignored. The consequences of this are discussed below.

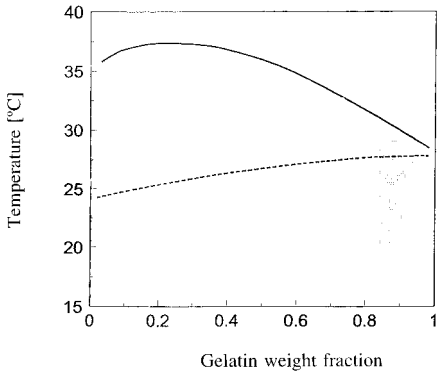

Figure 3. Schematic temperature/composition state diagram of an aqueous dextran/gelatin/0.5 M NaCl solution of a total polymer concentration of 7%: full line, coexistence line; dotted line, gel line. In the shaded area, the phase separation experiments have been carried out.

Experimental Section

At two compositions, I 0.5% dextran/9.2% gelatin and II 0.9% dextran/7.2% gelatin, the phase separation was studied with SALS and phase contrast microscopy at 21, 23, 25, and 29 °C in case I, and at 21, 23, 25, and 27 °C in case II. All these temperatures are below the phase separation temperature. The temperature ranges were chosen in order to straddle the gelation temperature of pure gelatin in 0.5 M NaCl, which is around 25 °C (see Figure 3).

Dextran (from *Leuconostoc mesenteriodes*) was purchased from Sigma Chemical. From wide angle light scattering the weight averaged molar weight (M_w) was found to be 160 000 g/mol. A range of well-characterized porcine skin gelatin fractions was kindly provided by Sanofi Bio-Industries. The M_w of the gelatin was 162 400 g/mol ($M_w/M_n = 2.4$). Dextran and gelatin were used without further purification. Solutions of gelatin and dextran in 0.5 M NaCl were made by adding dry solutes and solvent together. Stirring and heating to about 80 °C for 30 min resulted in clear solutions. The schematic state diagram at 7% total polymer concentration (Figure 3) shows the typical shape of the coexistence line for dextran/gelatin/0.5 M NaCl/water systems and was obtained as described in ref 4. A more detailed phase diagram of a closely related system can be found in ref 11. The phase separation of the 0.5% dextran/9.2%(gelatin w/w) and 0.9% dextran/7.2%

gelatin w/w) systems takes place between 30 and 35 °C. The phase transition temperature could not be determined more accurately, because of a very strong hysteresis.

A short account of the experimental procedure will be given here. For a more detailed description, see ref 4. The hot solution gelatin and dextran, well above the phase transition temperature, was pipetted into a sapphire crucible on the preheated hot stage of the SALS instrument. This sample was cooled at 20 °C/min to the temperature, below the phase transition temperature, where the phase separation and gelation process was to be observed. The changing scattering pattern was recorded at time intervals varying between 10 s and 10 min, depending on the rate of change. Because the scattered intensity was directly registered by a CCD camera, the scattering images are available with an absolute intensity scale, rendering feasible a detailed interpretation of the shape of the scattering pattern. For the calibration of the scattering angle and intensity scales, a pinhole was used. The 2-D scattering patterns were point symmetric, so radial averaging could be applied, resulting in an improved signal to noise ratio. During phase separation experiments, the transmission was estimated to be at least 90%. Such a high transmission is in accordance with the samples remaining unchanged to the eye. Therefore, multiple scattering effects were neglected.

The phase contrast microscopic image was obtained in the same way as in ref 4.

Results and Discussion

General. Figure 4 shows that the scattering pattern is reminiscent of that observed in spinodal decomposition. The maximum suggests a certain characteristic length scale in the concentration inhomogeneities after the onset of phase separation. The amplitude of the maximum increases, tentatively interpreted as a build up of concentration difference. However, it will turn out that such a interpretation is not necessarily right and that the situation in the present case of growing spherical regions surrounded by a depletion layer implies a complex relation between position and height of the maximum on the one hand and the size and density of the spheres on the other. Due to the broad peak shape, in particular for system I (Figure 4a), the position $q_m(t)$ of the maximum is badly defined in the experimental data and the plot of q_m versus time (Figure 5) is therefore noisy and of limited quantitave use. There appears to be no consistent power law behavior. Subtle changes in the shape of the peak superimpose patterns on the gradual time dependence of q_m. From considering the time dependence for system II of q_m and the peak height (Figures 5b, which is relatively low in noise, and 6b), it is seen that with a nearly stationary peak position, the peak height is growing close to an order of magnitude. This is a demonstration of the absence of dynamical scaling. This, together with the slow time dependence of q_m, would suggest that the systems is in the "transition regime", where, as mentioned before, power law growth has been predicted with exponents between $^1/_6$ and $^1/_3$. The stage of coarsening according to a $^1/_3$ power law dependence is not reached in the present systems during the time of observation.

Figure 4 shows also the fit of the model of Figure 1 to the scattering data at 23 °C of systems I and II at several times after the quench. It shows the typical quality of the fit. The high-q downward slope is well-reproduced, whereas there is a slight mismatch around the maximum. This will be ascribable to the simplicity of the model, in particular with regard to the way the depletion layer is represented. Also, the effect of ignoring polydispersity of the spheres may increase the mismatch. The limited number of data points does not allow for an additional adjustable parameter describing

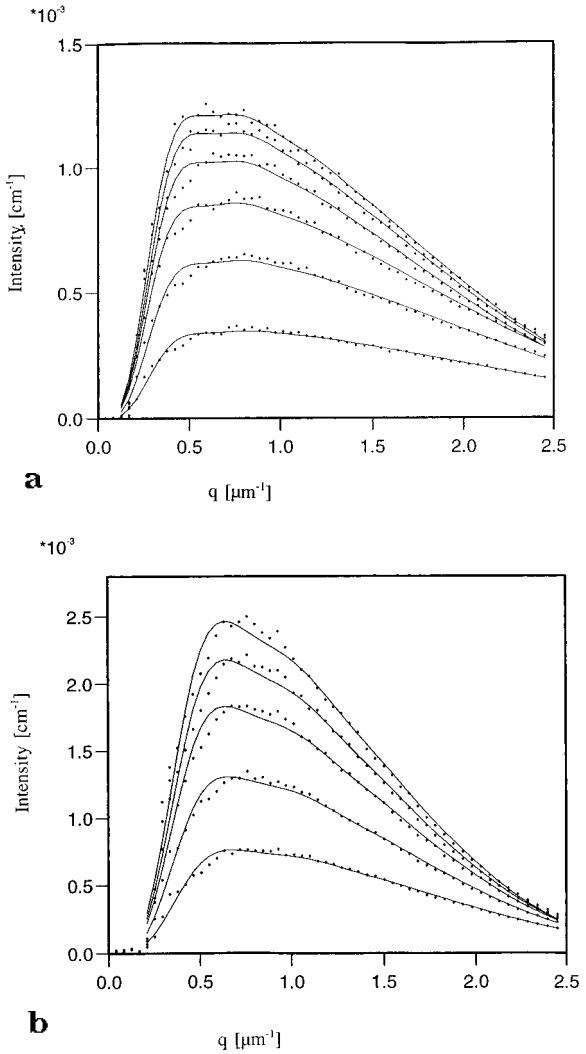

Figure 4. The development over time of the SALS pattern of (a) 0.5% dextran/9.2% gelatin and (b) 0.9% dextran/7.2% gelatin during 20 min after a quench to 23 °C. The phase separation temperature is between 30 and 35 °C; the gelation of gelatin takes place at about 25 °C. The full lines are the fits of eq 6.

polydispersity. The microscope image of composition I (Figure 2) shows some polydispersity. The effect of polydispersity is probably a broadening of the peak and may be significant. As a consequence of the simplicity of the model and the ignoring of polydispersity, the interpretation of the fit results will be qualitative rather than quantitative.

Fit Results. Figures 7, 8, and 9 show the results of fitting eq 6 to the data sets from the gelatin-rich systems at different temperatures. Because solution I has a total solute concentration that is higher than that of solution II, the temperature quenches for I are effectively deeper than for II. Figure 7 shows a growth of the core size r_1 of the dextran spheres, which turns out to be on the order of 1 μm in size, in agreement with the photographic observation. There are some signs that the growth approaches power law behavior at later times at temperatures above the gelation temperature of the gelatin matrix. The power is about 0.13. Below the gelation temperature, initial growth is followed by levelling off as a result of gelation of the surrounding matrix. The dependence of the sizes on temperature in solution I and in late stages in solution II is as would be expected from classic theory for homogeneous nucleation: the higher the temperature (i.e. the closer

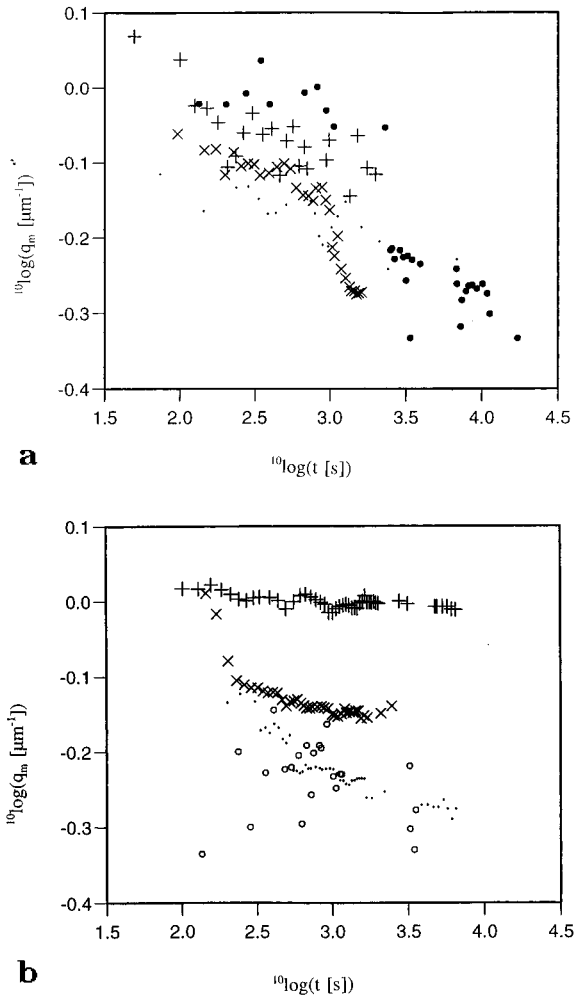

Figure 5. The position of the maximum q_m vs time in (a) 0.5% dextran/9.2% gelatin and (b) 0.9% dextran/7.2% gelatin. +, 21 °C; ×, 23 °C; •, 25 °C; ○, 27 °C; ●, 29 °C.

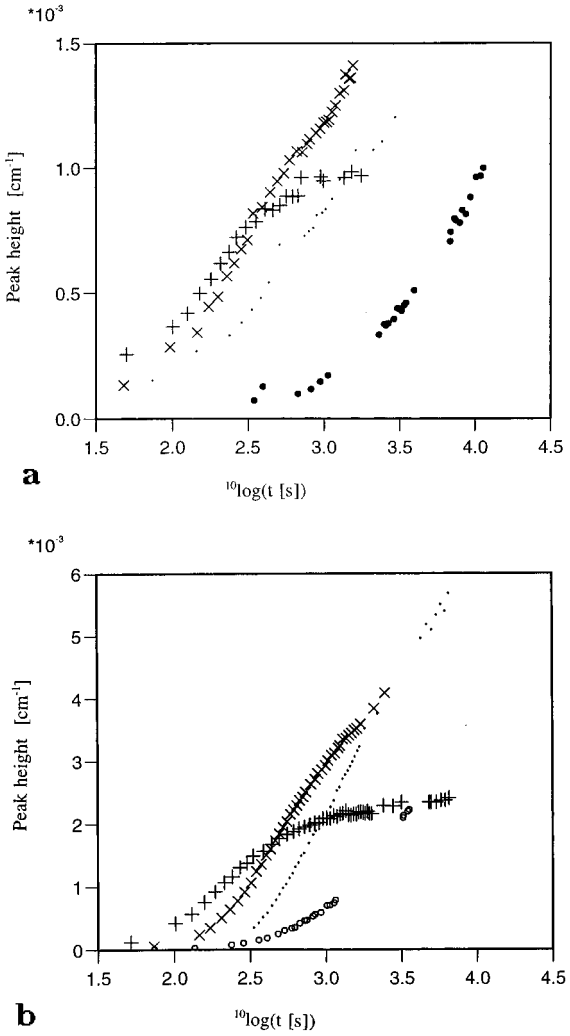

Figure 6. The amplitude of the scattering maximum vs time for (a) 0.5% dextran/9.2% gelatin and (b) 0.9% dextran/7.2% gelatin: +, 21 °C; ×, 23 °C; •, 25 °C; ○, 27 °C; ●, 29 °C.

to the coexistence line), the larger the critical size above which nuclei are stable and growing. In solution II the final arrangement of sizes according to temperature is only reached after a crossover from nearly the reverse arrangement. An explanation could be that the formation of dextran-rich regions is not initiated by homogeneous nucleation; instead, the nuclei form on impurities and their size is determined by the concentration of impurities, rendering arbitrary in initial stages the absolute size as a function of temperature. The growth is impeded by the gelation of the surrounding gelatin phase, resulting in a final size arrangement according to the gelation rate, which is expected to increase with decreasing temperature. Such an arrangement is indeed observed. Comparison of Figures 5 (q_m vs time) and 8 shows that, especially below the gelation temperature, the peak position is stationary, in spite of the fact that the spheres are growing. This underlines the difference between the present behavior of the scattering pattern and that of the scattering from near-critical phase separation, where a growing domain size is accompanied by a moving peak position.

Figure 8 shows that r_2, the thickness of the depletion layer, is typically 10 times r_1. Unfortunately, the behavior of r_2 cannot be interpreted quantitatively because of the arbitrary way in which r_2 enters the model. The choice of the functional shape of the depletion layer profile determines the value of r_2 that will be found. The observed trends, however, are more meaningful. At the lower temperatures, hardly any growth is observed. Only at 29 °C does the depletion layer turn out to be growing fast, which suggests that, at this high temperature, the phase separation is in an earlier stage, in which the depletion layer is still developing, whereas at the lower temperatures the size of the depletion layer has settled before observation started. The general trend in the temperature dependence of this settled depletion layer thickness is an increase with increasing temperature.

There is no strong time dependence in the density y (Figure 9), consistent with the well-defined spheres with apparently sharp interfaces observed under the microscope from the earliest stages on. The minor increase with time below the gelation temperature of the matrix is explained by the contraction of the gelatin matrix during gelation, enhancing the contrast between the dextran-rich and gelatin-rich phases. As expected, the density decreases with increasing temperature, because the higher the temperature, the smaller the difference between coexisting phases. In solution I the density is higher, which is in agreement with the fact that the phase separation takes place deeper under the coexistence line. From Figure 6, which shows the peak amplitudes as a function of time, it can be seen that the deeper quenched solution I has a lower maximum scattering intensity, in spite of the fact that the density of the dextran spheres is higher. Of course, the size of

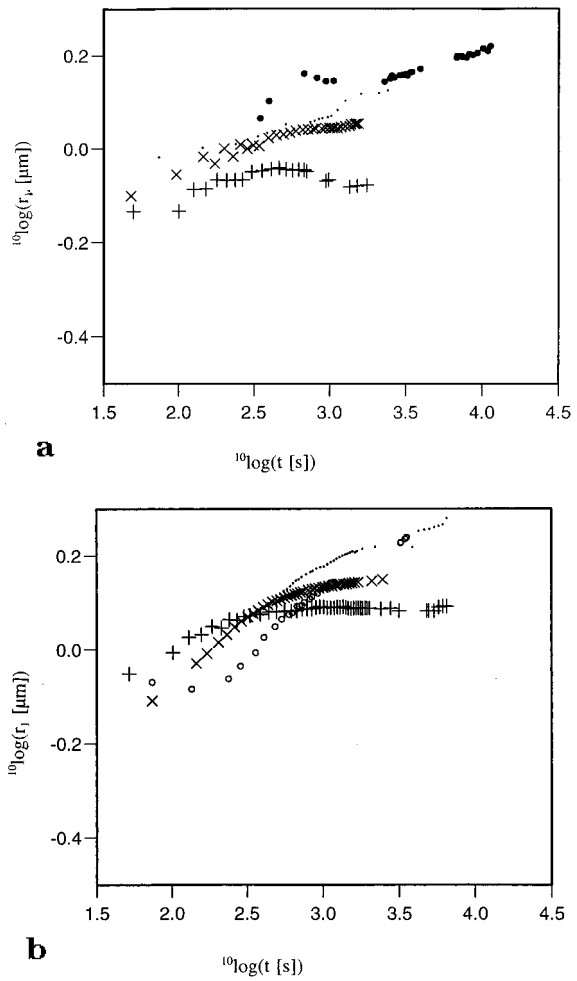

Figure 7. The radius of the sphere r_1 vs time for (a) 0.5% dextran/9.2% gelatin and (b) 0.9% dextran/7.2% gelatin: +, 21 °C; ×, 23 °C; •, 25 °C; ○, 27 °C; ●, 29 °C.

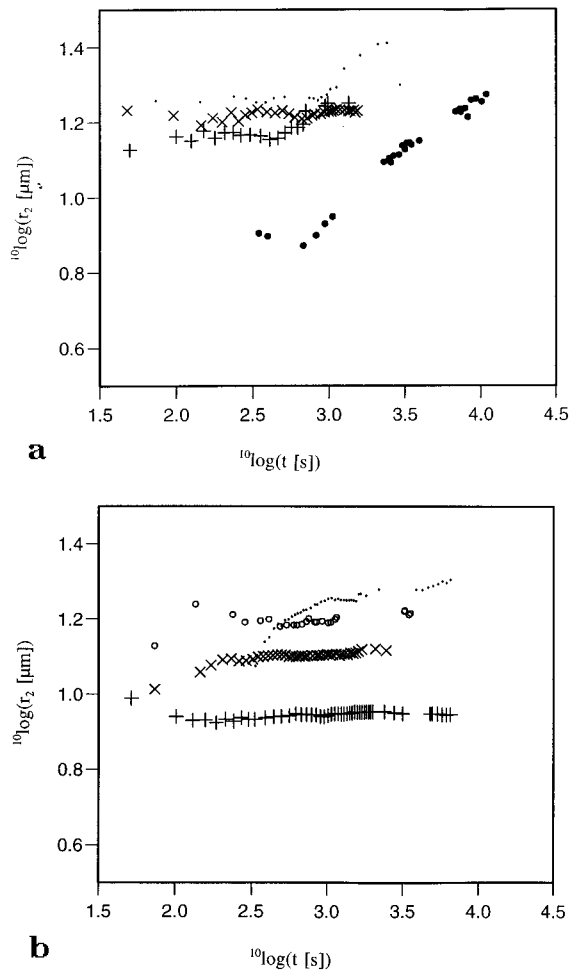

Figure 8. The radius of the depletion layer r_2 vs time for (a) 0.5% dextran/9.2% gelatin and (b) 0.9% dextran/7.2% gelatin: +, 21 °C; ×, 23 °C; •, 25 °C; ○, 27 °C; ●, 29 °C.

the spheres is another important factor determining the height of the scattering peak. Figure 10 demonstrates the effect of sphere size on the scattering peak amplitude. Here, the amplitude of the scattering maximum of solution II is plotted versus r_1^6. It turns out that for temperatures above the gelation temperature, the peak amplitude is proportional to the square of the accumulated volume. Surprisingly, the presence of a depletion layer does not affect a simple relationship between sphere size and peak height, similar to that between particle size and the first-order scattering maximum in dilute suspensions without depletion layers. The different slopes in Figure 10 reflect the varying densities at different depths under the coexistence curve.

The depth of the depletion layer d, calculated with eq 5, is plotted in Figure 11, in the same units as the density y. The absolute value of d is typically 1000 times smaller than that of y. As in the case of the depletion layer thickness r_2, the quantitative behavior of d is strongly dependent on the assumption of the model. The plotted quantity should therefore be regarded as roughly portional to the deviation directly outside the dextran sphere of the composition from its average value. In both solutions an initial deepening of the depletion is observed, followed by a levelling off in solution II and, at least for 21 and 25 °C, an upturn to less negative values in solution I. The depletion is stronger in solution II, the more dilute one, than in solution I, which is due to the slower gelation in solution II, leaving more time for a depletion to build up. Possibly, another factor is a larger diffusion constant of dextran in solution II, due to the lower overall concentration and less gelation. The depletion is stronger the lower the temperature, which reflects the initially faster phase separation process at temperatures further below the coexistence line. The bottoming out of the depletion, observed in solution I, is in agreement with the expectation that eventually the depletion should disappear, at least when no gelation of the surroundings takes place. The time at which the relaxation of the depletion sets in and the depth which the depletion has reached by that time will be a function of the phase separation rate, gelation rate, and mutual diffusion constant, all of which are temperature dependent. Therefore, the reason that no or very weak bottoming out of the depletion is observed in solution II may be that the phase separation process has not proceeded far enough, whereas in solution I the phase separation reached a further stage, in spite of the fact that the depletion is weaker.

Final Remarks. The general picture that emerges is initial growth of dextran-rich nuclei that is arrested by the gelation of the surrounding matrix when the temperature is low enough. Above the gelation temperature the growth continues. For gelling systems, the width of the depletion layer is constant as a function of time from the beginning of the observation period. By the time further growth of the spheres is prevented by gelation, the depletion layers have not shrunk. Conse-

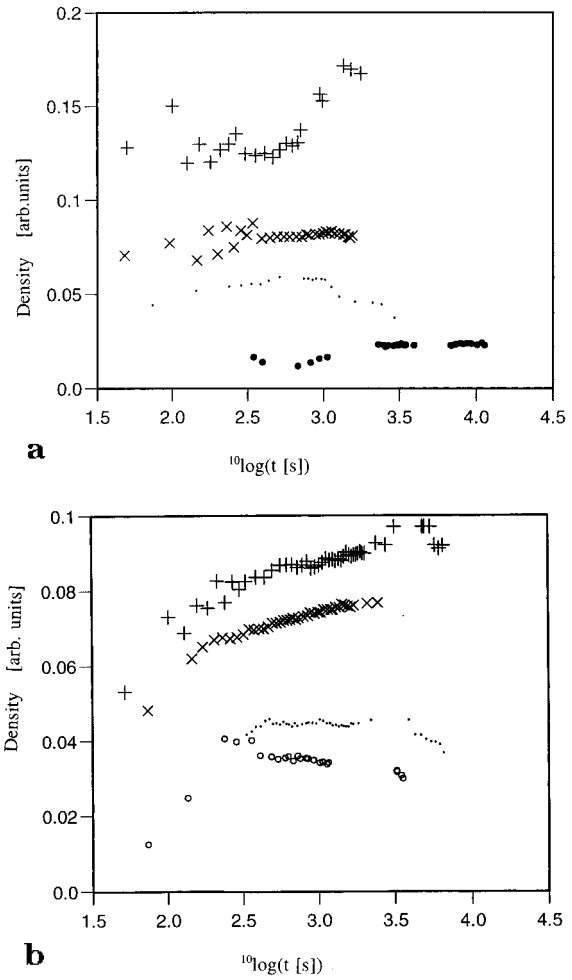

Figure 9. The density of the sphere y (on a linear scale) vs time for (a) 0.5% dextran/9.2% gelatin and (b) 0.9% dextran/7.2% gelatin: +, 21 °C; ×, 23 °C; ·, 25 °C; ○, 27 °C; ●, 29 °C.

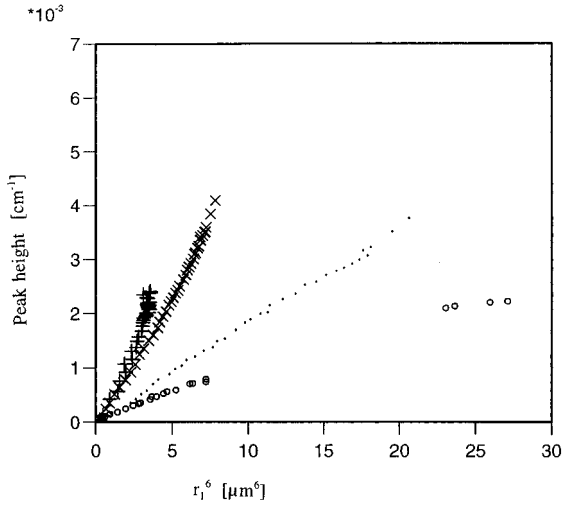

Figure 10. The peak amplitude vs the square of the sphere volume r_1^6 for 0.9% dextran/7.2% gelatin: +, 21 °C; ×, 23 °C; ·, 25 °C; ○, 27 °C.

quently, the gelatin matrix in the gelled dextran/gelatin matrix has an inhomogeneous composition that will affect the macroscopic mechanical properties. With regard to the cause of the constant value of the depletion layer thickness, two suggestions can be made: it may be due to the gelation of the matrix, which prevents further growth of the depletion layer. Such a "frozen" depletion layer size is in clear contradiction with the observations of growing spheres and deepening of the

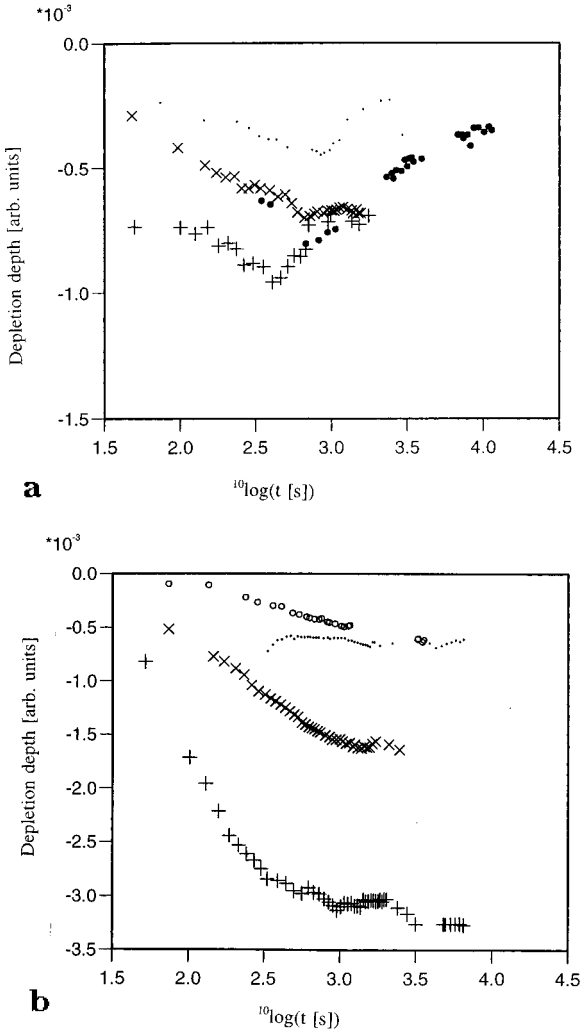

Figure 11. The depletion depth d vs time for (a) 0.5% dextran/9.2% gelatin and (b) 0.9% dextran/7.2% gelatin: +, 21 °C; ×, 23 °C; ·, 25 °C; ○, 27 °C; ●, 29 °C.

depletion. Moreover, macroscopic gelation is only observed at least 10 min after even the deepest quench to 21 °C. More plausibly, the sizes of the depletion layers had already reached their maximum value, i.e. where they start to touch the neighboring depletion layers, by the time the observation began. Such a situation would imply perhaps the most important shortcoming of the present simple model: the ignoring of the interaction between the depletion layers of neighboring dextran spheres, growing in a gelatin matrix. The profile in Figure 1 assumes a vanishing depletion at r_2, whereas it actually may have a nonzero value. Unfortunately, far more detailed scattering patterns are needed to cope with the (at least one) extra parameter needed to introduce particle concentration in a model profile.

With the simple profile used in this work to interpret the light-scattering patterns, some trends in the structural parameters have been obtained that are fairly easily understood. On these grounds, it is believed that this model offers a good starting point for obviously needed refinements.

Conclusions

The growth of dextran-rich spheres was followed as part of the phase separation process in off-critical aqueous mixtures of gelatin and dextran, with gelatin as the majority phase. The SALS pattern turned out

to be consistent with a dense nucleus, surrounded by a depletion layer. At temperatures above the gelation temperature of gelatin, growth of the spheres was observed during the entire observation period (up to 4 h), whereas below the temperature of gelation of the gelatin matrix, growth was arrested by the gelation. The growth of the spheres is accompanied by an initial deepening of the depletion layer, which is in some cases followed by a relaxation of the depletion. The density of the spheres, as reflected by their scattering strength per unit volume, depends on temperature and total polymer concentration in a way expected from the phase diagram. The contrast (scattering strength) of the spheres increases on gelation of the gelatin matrix, due to contraction of the gelatin phase. From the independence of the thickness of the depletion layer on time, it is concluded that right from the beginning of the observation period (100 s after the temperature quench) depletion layers are extending toward those of the neighboring spheres. Therefore, in the final, gelled state of the system, concentration gradients fill the entire volume of the gelatin matrix.

Acknowledgment. We gratefully acknowledge Dr. Adrian R. Rennie and Dr. Stuart Clarke, for stimulating discussions and technical support, and Sanofi Bio-Industries, for providing well-documented gelatin samples. The work was funded by a BBSRC grant.

References and Notes

(1) For example: *Cereals in Breadmaking*; Eliasson, A.-C., Larsson, K., Eds.; Marcel Dekker, Inc.: New York, 1993.
(2) Petrak, K. L. *J. Appl. Polym. Sci.* **1984**, *29*, 555.
(3) *Food Texture and Rheology*; Sherman, P., Ed.; Academic Press: London, 1979.
(4) Tromp, R. H.; Rennie, A. R.; Jones, R. A. *Macromolecules* **1995**, *28*, 4129.
(5) Gyure, M. F.; Harrington, S. T.; Strilka, R.; Stanley, H. E. *Phys. Rev. E* **1995** *52*, 4632.
(6) Nakazawa, H.; Sekimoto, K. *J. Chem. Phys.* **1996** *104*, 1675.
(7) Carpineti, M.; Giglio, M.; Degiorgio, V. *Phys. Rev. E* **1995**, *51*, 590.
(8) Banfi, G.; Degiorgio, V.; Rennie, A. R.; Barker, J. G. *Phys. Rev. Lett.* **1992**, *69*, 3401.
(9) Binder, K.; Stauffer, D. *Adv. Phys.* **1976**, *25*, 343; Wagner. R.; Kampmann, R. *Mater. Sci. Technol.* **1991**, *5*, 213.
(10) Tanaka, H. *Phys. Rev. Lett.* **1993**, *71*, 3158.
(11) Durrani, C. M.; Prystupa, D. A.; Donald, A. M.; Clark, A. H. *Macromolecules* **1993**, *26*, 981.

MA9606566